Journal of Medicinal Chemistry

Article

Overcoming Mutagenicity and Ion Channel Activity: Optimization of Selective Spleen Tyrosine Kinase Inhibitors

J. Michael Ellis, Michael D Altman, Alan Bass, John W Butcher, Alan J Byford, Anthony Donofrio, Sheila Galloway, James Jewell, Andrew M. Haidle, Nancy Kelly, Erica K Leccese, Sandra Lee, Matthew L Maddess, J Richard Miller, Lily Y Moy, Ekundayo Osimboni, Ryan D Otte, M Vijay Reddy, Kerrie Spencer, Binyuan Sun, Stella H. Vincent, Gwendolyn J Ward, Grace HC Woo, Chiming Yang, Hani Houshyar, and Alan B. Northrup

Just Accepted

1
2
3
4
5
6
7
8
9
10
11
12
13
14
15
16
17
18
19
20
21
22
23
24
25
26
27
28
29
30
31
32
33
34
35
36
37
38
39
40
41
42
43
44
45
46
47
48
49
50
51
52
53
54
55
56
57
58
59
60

SCHOLARONE™
Manuscripts

Overcoming Mutagenicity and Ion Channel Activity:

Optimization of Selective Spleen Tyrosine Kinase

Inhibitors

J. Michael Ellis,[a]* Michael D. Altman,[a] Alan Bass,[f] John W. Butcher,[a] Alan J. Byford,[d] Anthony

Donofrio,[a] Sheila Galloway,[f] Andrew M. Haidle,[a] James Jewell,[a] Nancy Kelly,[d] Erica K.

Leccese,[d] Sandra Lee,[a] Matthew Maddess,[b] J. Richard Miller,[d] Lily Y. Moy,[d] Ekundayo

Osimboni,[a] Ryan D. Otte,[a] M. Vijay Reddy,[f] Kerrie Spencer,[a] Binyuan Sun,[a] Stella H. Vincent,[e]

Gwendolyn J. Ward,[f] Grace H. C. Woo,[a] Chiming Yang,[g] Hani Houshyar,[c] Alan B. Northrup[a]

Departments of Discovery Chemistry, Immunology, Pharmacology, Pharmacokinetics,

Pharmacodynamics, and Drug Metabolism, Safety Assessment and Laboratory Animal

Resources, and Discovery Pharmaceutical Sciences, Merck & Co., Inc., 33 Avenue Louis

Pasteur, Boston, MA 02115

[a]Department of Discovery Chemistry

[b]Department of Process Research

[c]Department of Immunology

[d]Department of Pharmacology

[e]Department of Pharmacokinetics, Pharmacodynamics, and Drug Metabolism

[f]Department of Safety Assessment and Laboratory Animal Resources

[g]Department of Discovery Pharmaceutical Sciences

Spleen Tyrosine Kinase. Ames. Mutagenicity. Ion Channels.

Abstract

Development of a series of highly kinome selective Spleen Tyrosine Kinase (Syk) inhibitors with favorable drug-like properties is described. Early leads were discovered through X-ray crystallographic analysis, and a systematic survey of cores within a selected chemical space focused on ligand binding efficiency. Attenuation of hERG ion channel activity inherent within the initial chemotype was guided through modulation of physicochemical properties including logD, PSA, and pKa. PSA proved most effective for prospective compound design. Further profiling of an advanced compound revealed bacterial mutagenicity in the Ames test using TA97a *Salmonella* strain, and subsequent study demonstrated that this mutagenicity was pervasive throughout the series. Identification of intercalation as a likely mechanism for the mutagenicity enabled modification of the core scaffold. Implementation of a DNA binding assay as a pre-screen and models in DNA allowed resolution of the mutagenicity risk, affording molecules with favorable potency, selectivity, pharmacokinetic, and off-target profiles.

Introduction

The utility of kinase inhibitors in treating oncological disorders was affirmed by the approval of imatinib in 2001.[1] In recent years, small molecule inhibitors of protein kinases have been examined for use in various autoimmune disorders, including rheumatoid arthritis (RA).[2] RA is a systemic inflammatory disorder that affects ~1% of the worldwide population with women three times more likely than men to develop the disease.[3] Disease progression is characterized by

synovial hyperplasia, inflammation, and irreversible joint destruction. This commonly leads to disability and consequent reduction in the quality of life and, if untreated, reduces life expectancy in patients. The pathogenesis of RA consists of a cascade of pro-inflammatory cytokines and chemokines leading to the recruitment of inflammatory cells. Traditionally, T cells, macrophages, neutrophils, and synovial fibroblasts were thought to be associated with RA;[4] however, current evidence suggests that autoreactive B cells, immune complexes, osteoclasts, mast cells, and basophils also contribute to the disease.[5]

Current therapies used to treat RA generally fall into two broad categories: palliative therapies and disease-modifying agents. Palliative therapies are prescribed to provide symptomatic relief from the pain and inflammation characteristic of RA. Disease-modifying therapies including conventional disease-modifying antirheumatic drugs (DMARDs) and biologic agents are prescribed to halt the destructive course of RA and prevent debilitating joint damage. Despite their success, the use of conventional DMARDs and biologics is limited by non-response in a subset of patients, safety concerns, and the high cost and discomfort of continuous injections with biologics. The 2012 approval of tofacitinib, an oral pan-Janus kinase (JAK) inhibitor, for treatment of RA cases that are inadequately responsive to methotrexate provides proof of concept for the therapeutic approach of kinase inhibition for the treatment of RA.[6]

Spleen tyrosine kinase (Syk) is a key enzyme involved in Fc and B cell receptor (BCR) signaling in multiple cell types involved in the immune response.[7] Inhibition of Syk activity is expected to slow the destructive course of RA by affecting the initiation phase via modulation of signaling downstream of the BCR, the effector phase via blockade of the Fc receptors (FcεR, FCγR) in various immune cells in the synovium, and the ensuing tissue damage via inhibition of osteoclast maturation.[8] Multiple preclinical studies have shown that genetic depletion of Syk or

inhibition of Syk with small molecule inhibitors (including published R788 (**1**), PRT-062607 (**2**), RO9021 (**3**), and GS-9973 (**4**)) attenuates inflammation, tissue damage and bone destruction in preclinical RA models (Figure 1).[9,10,11,12] Human proof-of-concept has been achieved in RA clinical trials with the poorly selective oral Syk inhibitor **1** (52% of 100 kinases tested >100X Syk IC$_{50}$).[13] Additional human proof-of-biology has been established with the B-cell depletion therapy Rituximab, approved for the treatment of RA.[14] Dosing with **1** in humans was limited by hypertension and diarrhea as the most common adverse events. We hypothesized that the hypertension observed was driven by off-target activity[15] and sought to develop a selective Syk inhibitor for the treatment of various autoimmune and hematological diseases, including RA, oncology,[16,17] and asthma,[18,19] devoid of this undesired pharmacology. This manuscript describes the preparation of diaminocarboxamides that are highly selective, potent Syk inhibitors as well as details regarding the attenuation of inherent hERG ion channel activity and mutagenicity risk within the chemotype to ultimately afford novel Syk inhibitors with favorable overall profiles.

Figure 1. Diverse Syk Inhibitor Motifs from the Literature.

Fostamatinib, R788 (**1**)   PRT-062607 (**2**)   RO-9021 (**3**)   GS-9973 (**4**)
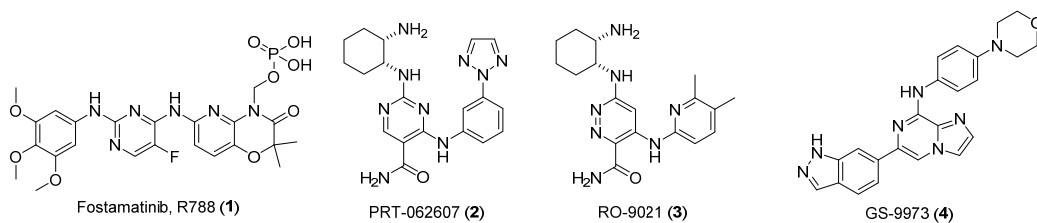
Chemistry

The main two points of structure activity relationship diversity for the aminodipyridylcarboxamides were in the basic amine region and the aminoheterocycle (solvent front) region. We developed modular approaches allowing late stage introduction of each of these functionalities (Scheme 1). Namely, the basic amine portion of the molecule could be introduced first starting from a dihalopyridyl nitrile under S$_N$Ar or palladium-mediated

conditions. As an example of the former method, the synthesis of picolinamide **5** commenced via reaction of 3-bromo-5-fluoropyridine-2-carbonitrile (**6**) and *tert*-butyl [(1*S*,2*R*)-2-aminocyclohexyl]carbamate mediated by base to afford bromide **7** in 82% yield. Introduction of 2-amino-4,6-dimethylpyridine was accomplished under Buchwald–Hartwig conditions in high yield.[20] Alkaline peroxide promoted the hydrolysis of nitrile **8** to the corresponding amide, which was subsequently deprotected under acidic conditions and free-based with ammonia in methanol to provide carboxamide **5** in 84% yield over three steps.

Alternatively, picolinamide **9** was prepared using the latter method of early-stage aminoheterocycle introduction. Anionic addition of 4,6-dimethylpyridin-2-amine to 5-bromo-3-fluoropicolinonitrile (**10**) gave bromopyridine **11**. Palladium-mediated coupling of *tert*-butyl (1-(aminomethyl)cyclopropyl)carbamate gave diaminopyridine **12**, which was further functionalized via acidic deprotection and hydrolysis to afford carboxamide **9**.

Scheme 1. Synthesis of *N*-linked heterocycles.
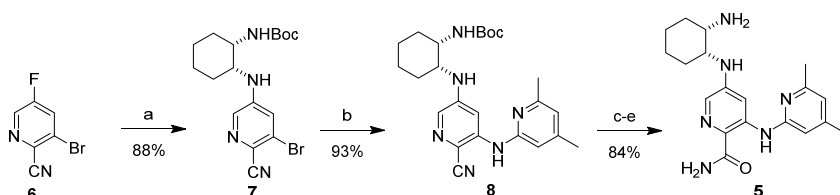
(a) *tert*-butyl [(1*S*,2*R*)-2-aminocyclohexyl]carbamate, DIEA, 110 °C; (b) 2-amino-4,6-dimethylpyridine, Pd$_2$(dba)$_3$, Xantphos, Cs$_2$CO$_3$, dioxane, 80 °C; (c) NaOH, 35% aq. H$_2$O$_2$, DMSO, rt; (d) HCl, dioxane; (e) NH$_3$, MeOH, rt.

Scheme 2. Alternative approach to the synthesis of *N*-linked heterocycles.
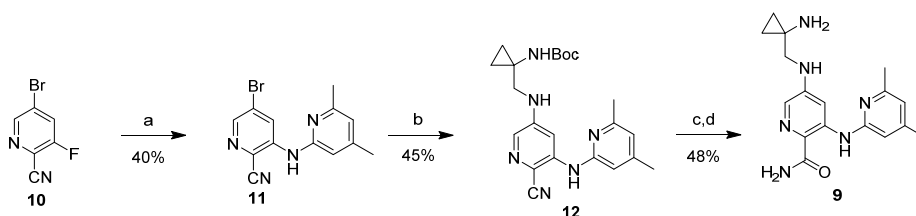
(a) 2-amino-4,6-dimethylpyridine, KO-*t*-Bu, THF, 0 °C;   (b) *tert*-butyl (1-(aminomethyl)cyclopropyl)carbamate, Pd$_2$(dba)$_3$, Xantphos, Cs$_2$CO$_3$, dioxane, 80 °C; (c) TFA, CH$_2$Cl$_2$, rt (d) NaOH, 35% aq. H$_2$O$_2$, DMSO, rt.

For the later generation *C*-linked carboxamides, a modified synthetic approach was employed.

As an exemplar, preparation of **13** commenced via S$_N$Ar addition of *tert*-butyl ((1*S*,2*R*)-2-aminocyclohexyl)carbamate and 2,6-dichloropyrazine (**14**) to give chloropyrazine **15** in 88% yield. Iodination *para* to the newly installed amine was accomplished using *N*-iodosuccinimide to afford dihalopyrazine **16** in 91% yield. Carefully monitored cyanation under palladium-mediated conditions provided nitrile **17** in 83% yield, which was subsequently functionalized via a Suzuki–Miyaura coupling to install the indole moiety.[21] Deprotection and hydrolysis of the nitrile **18** delivered carboxamide **13** in 48% yield over three steps.

Scheme 3. Synthesis of *C*-linked heterocycles.
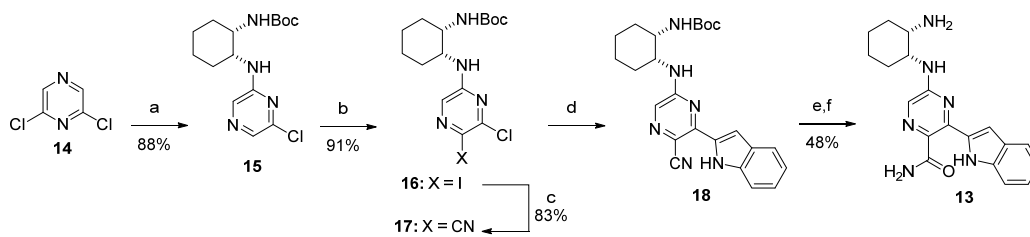
(a) *tert*-butyl [(1*S*,2*R*)-2-aminocyclohexyl]carbamate, DIEA, 115 °C; (b) NIS, DMF, 65 °C; (c) Zn(CN)$_2$, Pd(PPh$_3$)$_4$, DMF, 120 °C; (d) 1*H*-indole-2-boronic acid pinacol ester, Pd(OAc)$_2$, PCy$_3$, K$_2$CO$_3$, THF, 65 °C; (e) TFA, CH$_2$Cl$_2$, rt; (f) KOH, 35% aq. H$_2$O$_2$, DMSO, rt.

Results and Discussion

Our primary medicinal chemistry goal was to identify a highly kinome selective molecule that demonstrated favorable properties for further development activities. Carboxamide scaffolds (e.g. PRT-062607) were known in the literature at the outset of our efforts as potent Syk inhibitors. Examining the available structural and crystallographic data for Syk revealed Asp-512

as a key residue to target for selectivity enhancement.[22] Namely, an appropriately positioned array of hydrogen bond donors, such as the diamine present in YM-70220, had been demonstrated to recruit Asp-512 toward the ATP site, affording improved kinome selectivity as this motion of the catalytic Asp is unfavorable for a number of kinases (Figure 3).[23] Having settled upon Asp-512 as a key point of interaction, we next undertook a systematic core scan of diaminocarboxamides (Table 1). Our objective was to ensure a high ligand efficiency for Syk, while obviating the presence of a potentially reactive aniline substructure, which has been reported to increase risk for toxicity.[24] Generally, ligand efficiencies were in an acceptable range for all permutations tested (0.42–0.56); structure activity relationships revealed that aryl carboxamides possessing nitrogen *ortho* to the carboxamide were beneficial to potency (picolinamide **5** vs. benzamide **19**), while a nitrogen at the *meta* position was deleterious to potency (benzamide **19** vs. nicotinamide **20**).[25] We hypothesized that an intramolecular hydrogen bond between the amide NH and the heteroaryl nitrogen served to pre-organize the ground state conformation in a planar geometry stabilizing the bioactive conformation as well as lower the penalty for desolvation (**23** versus **24**, Figure 2). In contrast, an antagonistic steric interaction between the NH of the amide and the CH *ortho* to the amide is present in chemotypes lacking this heteroaryl nitrogen. Further, we proposed that the *meta*-nitrogen present in nicotinamide **20** and pyridazinecarboxamide **21** favors a ground state diamine conformation that requires a 180° rotation for recruitment of Asp-512 in the bioactive conformation (**25** versus **26**). Picolinamide **22** demonstrated an antagonistic interaction between the aniline solvent front and the picolinamide core resulting in a 100-fold intrinsic potency loss versus picolinamide **5** (**27** versus **28**). The potency advantage of the aminodipyridine was aligned with our strategy to avoid

anilines. With this data set, we chose to focus our efforts on the 3,5-diaminopicolinamides represented by compound **5**.

Table 1. Carboxamide Core Scan: Enzyme Potency and Ligand Binding Efficiency (LBE).

Analog	Structure	Syk IC$_{50}$ (nM)	LBE
19		2.8	0.47
20		19	0.42
5		0.06	0.56
21		4.7[b]	0.45[b]
22		8.8	0.43

[a]See supporting information for details. [b]See reference 25.

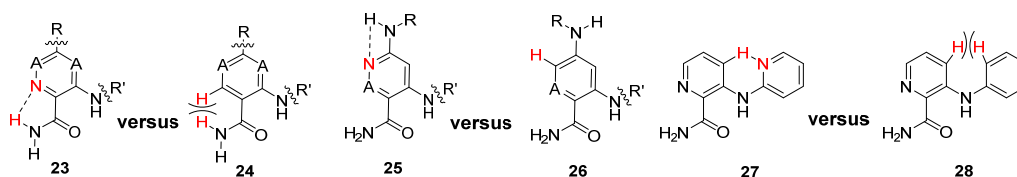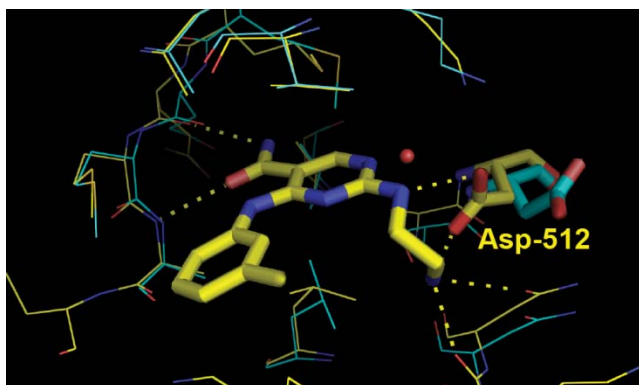**Figure 2.** Rationale for Intrinsic Potency Differences Across Cores.

Figure 3. Interaction of Basic Amine with Asp-512 for Syk Potency and Selectivity. X-ray Co-crystal Structure of YM-70220 in Syk (Yellow) Overlayed with AMP-PMP Structure with Syk (Cyan).

Further profiling of representative 3,5-diaminopicolinamide **5** revealed a number of favorable aspects; high enzymatic (Syk IC_{50} = 60 pM) and human whole blood potency (hWB CysLT IC_{50} = 58 nM) had been achieved, along with exquisite kinome selectivity (100% of 265 kinases tested >100X Syk IC_{50}). Carboxamide **5** also demonstrated high enzymatic selectivity versus the homologous enzyme Zeta-chain-associated protein kinase 70 (Zap70) with an IC_{50} of 5.3 nM (Zap70 IC_{50}/Syk IC_{50} = 90X).[26] Further, the physicochemical properties (HPLC logD = 2.1, PSA = 118) and oral pharmacokinetic profile (Rat Plasma Cl_p (Cl_u) = 33 (710) mL/min/kg, Rat $T_{1/2}$ = 2.7 h, F = 19%) of this molecule were in a desirable range.[27] Picolinamide **5** was profiled in the rat collagen induced arthritis model and demonstrated therapeutic efficacy at doses as low as 3 mg/kg QD PO (C_{max} = 0.2 μM, C_{min} = 0.007 μM, Figure 4). However, a key off-target activity of compound **5** was inhibition of the human Ether-a-go-go Related Gene (hERG, I_{Kr} IC_{50} = 1.6 μM). Several strategies have proven effective in the medicinal chemistry literature for attenuating delayed rectifying potassium channel activity including modulation of basicity and polarity.[28] We targeted the diamine and aminoheterocycle directed toward the solvent front for

modification in an attempt to merge the favorable properties of carboxamide **5** with weaker ion channel activity.

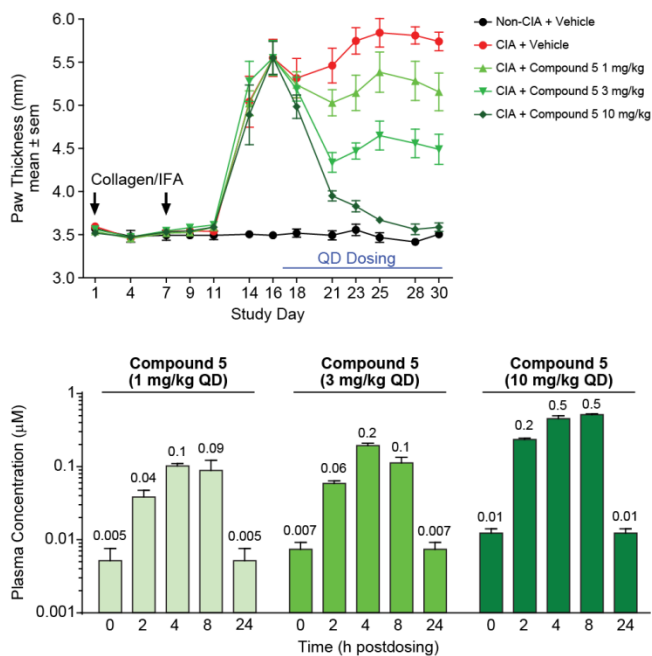**Figure 4.** Rat Collagen Induced Arthritis Efficacy of 3,5-diamino picolinamide **5**.
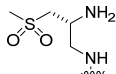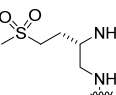

Table 2 details a systematic survey of the diamine portion of the molecules while holding the 2-amino-4,6-dimethyl pyridine constant. A number of calculated and measured properties were then leveraged to examine correlations between each category of properties and the corresponding hERG ion channel activities. A good correlation has been established in the literature, and was recapitulated with these chemotypes, between an automated patch clamp system, PatchXpress, and a higher throughput binding assay for measuring or estimating I_{Kr} IC_{50} values.[29,30] It is well-precedented that attenuation of amine basicity can result in weaker delayed rectifying potassium channel binding.[31] To maintain good Syk potency, it was important to avoid rendering the diamine non-basic at physiological pH (e.g. **29** and **33**). Calculated and/or measured pKa's above 7.0 showed little to no correlation with ion channel activity as measured

10

via PatchXpress (Figure 5). There was also a lack of correlation between measured HPLC logD

and I_{Kr} activity within a logD range of 0.7 and 2.3, though it did trend slightly in the expected

direction with more polar molecules showing lower ion channel binding (Figure 5). The most

robust correlation was found between polar surface area (PSA) and hERG ion channel activity,

as a higher PSA biased molecules toward weaker activity, while maintaining Syk potency (**32**).

The diamino-tetrahydrothiopyran dioxide identified from this survey and exemplified in

picolinamide **32** emerged as a preferred moiety for interacting with Asp-512 while maintaining

potency (Syk IC_{50} = 0.1 nM), reasonable kinome selectivity (100% of kinases >100X, 265

kinases tested), and an improved off-target profile (hERG, I_{Kr} IC_{50} = 29 μM).

Table 2. Amine Region hERG Ion Channel SAR.
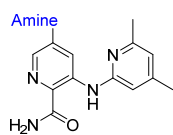
Analog	Amine	Syk IC_{50} (nM)[a]	Measured pKa	HPLC LogD	PSA[b]	I_{Kr} IC_{50} (μM)
5		0.06	9.0	2.1	118	1.6
29		7	7.2[c]	2.1	122	5.2
30		371	5.1	2.6	123	42[d]
9		0.5	7.9	1.9	124	1.7
31		0.8	7.8	1.4	135	1.6
32		0.1	7.0	1.5	157	29

33		184	5.7	1.2	160	>60[d]
34		5	8.3[c]	0.9	161	14

[a]See supporting information for details. [b]Polar surface area. [c]Calculated pKa. [d]MK-499 displacement IC$_{50}$ (µM).

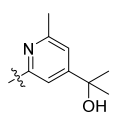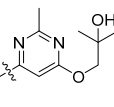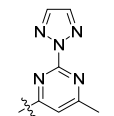**Figure 5.** Physicochemical Properties versus hERG Ion Channel Activity.
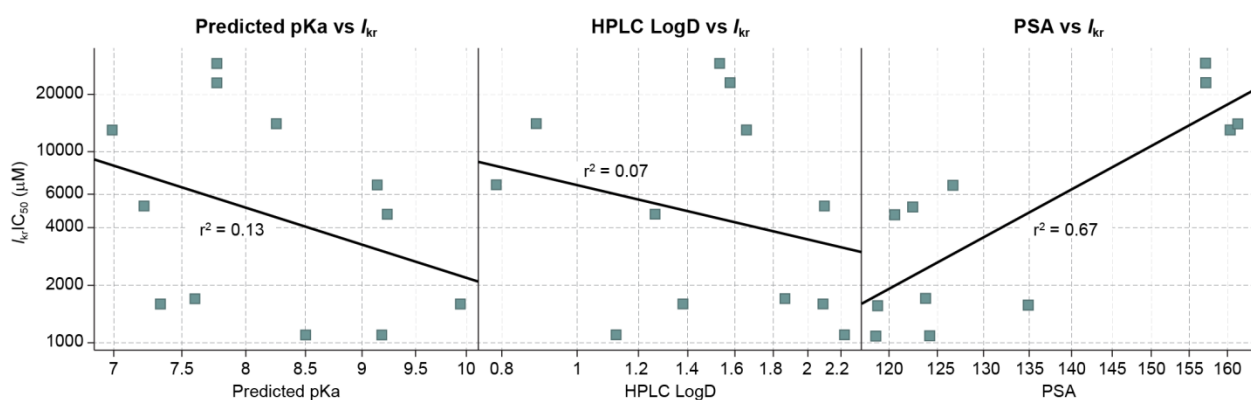
Efforts were next directed toward examining the impact of the aminoheterocycle directed toward the solvent front on hERG ion channel activity. In this case, the cyclohexyldiamino group was held constant to ensure a sufficient dynamic range for assessing the impact of the heterocycle. Again, polarity emerged as the key driver, as both measured HPLC logD and calculated PSA demonstrated strong correlations with hERG interaction. Namely lower HPLC logD (<1.0) and higher PSA (>145) effectively ablated potent I_{Kr} activity in the absence of attenuated diamine basicity. Having demonstrated the impacts of PSA across two distinct portions of the molecules on ion hERG activity, planning of future molecules was guided by calculation of this physicochemical property. This prospective analysis allowed rapid triage and prioritization of novel inhibitor designs. In short order, picolinamide **42** was synthesized and demonstrated a favorable overall profile. Carboxamide **42** was a potent and selective Syk

inhibitor (Syk IC_{50} = 0.6 nM, 99% of kinases >100X, 265 kinases tested, BLK IC_{50} = 32 nM, ROS IC_{50} = 43 nM) that demonstrated good cell and functional activity (hWB CysLT IC_{50} = 56 nM) lacking the ion channel activity of previous prototypes (hERG, I_{Kr} IC_{50} >30 µM). Though **42** has a higher calculated PSA (PSA = 167) than many drug-like molecules (typically PSA ≤140 for oral bioavailability), a favorable pharmacokinetic profile in preclinical species was obtained, including oral exposure (Rat Plasma Cl_p (Cl_u) = 19 (270) mL/min/kg, Rat $T_{1/2}$ = 2.8 h, 30 %F). The calculated PSA is believed to be an overestimate due to the extensive intramolecular hydrogen bonding network within the ground state of the molecule that serves to mask some of the inherent polarity from a topological assessment.

Table 3. Solvent Front hERG Ion Channel SAR.
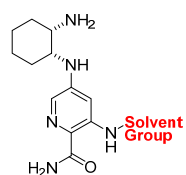
Analog	Solvent Group	Syk IC_{50} (nM)[a]	HPLC LogD	PSA[b]	I_{Kr} IC_{50} (µM)
5		0.06	2.1	118	1.6
35		0.5	2.2	118	0.6
36		0.8	1.7	130	1.7
37		0.1	1.4	138	1
38		0.9	1.3	138	5.9

39		9	1.2	139	6.5
40		0.2	1.0	158	18
41		0.01	0.9	162	44

aSee supporting information for details. bPolar surface area.

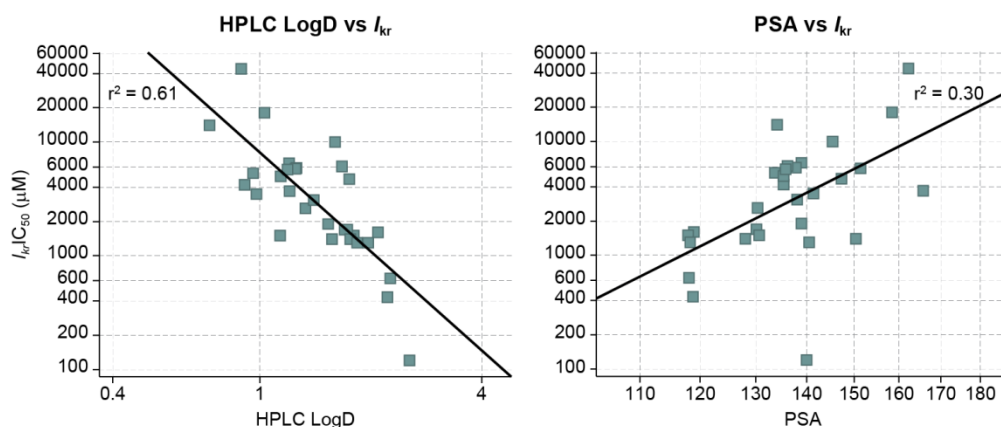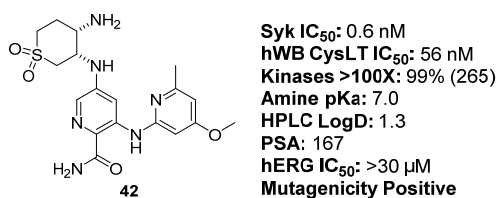**Figure 6.** Physicochemical Properties versus hERG Ion Channel Activity

Figure 7. Profile of Picolinamide **42**.

Syk IC$_{50}$: 0.6 nM
hWB CysLT IC$_{50}$: 56 nM
Kinases >100X: 99% (265)
Amine pKa: 7.0
HPLC LogD: 1.3
PSA: 167
hERG IC$_{50}$: >30 µM
Mutagenicity Positive

While preparing carboxamide **42** to move toward development, a report appeared in the literature of mutagenicity in the bacterial reverse mutation (Ames) test for a molecule of a similar chemotype, GSK-143 (**43**).[32] The report described a positive Ames test result for pyrimidinecarboxamide **43** in *Salmonella typhimurium* strain TA1537 without metabolic activation (Figure 8). Mutation in this strain often reflects intercalation of the test molecule into

14

DNA, and such activity can also be detected in *Salmonella* strains TA97 and TA97a which are considered equally acceptable with TA1537 under international test guidelines.[33] Since TA97a is the strain we use routinely, we selected this strain when carrying out a minimal screen, and performed the mutation testing in the presence of rat S-9 because the mutagenicity of **43** and some other candidates was enhanced by S-9 in our hands, and potential mutagenicity of aromatic amine metabolites (see below) would require metabolic activation. Our lead compound **42**, induced mutation in strain TA97a in the presence of rat S9.. Similarly, picolinamide **5** was tested, and showed a positive result at ≥ 300 µg/plate. Speculating that a metabolite could be the culprit in these results, we prepared and tested two potential degradative products. Diaminopyridine **45** had been found as a *N*-dealkylative metabolite in rat and human hepatocyte MetID studies. This molecule was predicted by DEREK for Windows (version 12.5.4, Lhasa Ltd., Leeds, UK) and Multi-CASE (MC4PC version 2.3.0.15, Multi-CASE Inc., Ohio, USA) to be positive in the Ames test due to the known mutagenic substructure of the primary aromatic amine in **45** (anilines **46** and **47** are known Ames positive compounds that feature this motif). However, the assay in strain TA97a was negative for **45** up to 3000 µg/plate with rat S9. Tricycle **44** had been observed to form upon standing with acid and could have been a prime suspect for intercalation. However, this compound was also negative in in TA97a with S9 up to 3000 µg/plate. With these results in hand, we began to formulate hypotheses to overcome the putative intercalation liability within this series.

**Figure 8.** Initial Compounds for Mutagenicity Assessment.
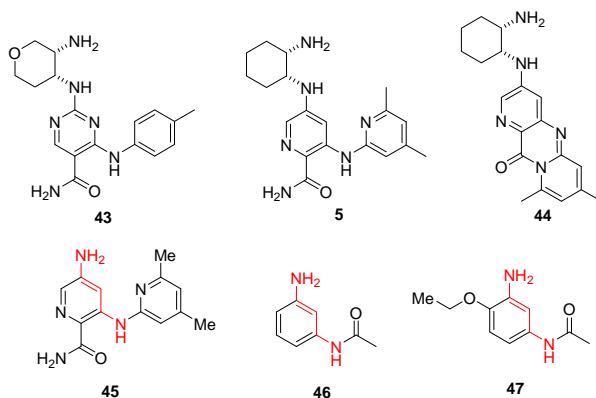
Leveraging DNA co-crystals with acridine, a docking model was developed for our Syk inhibitors (represented by picolinamide **5**) in DNA (Figure 9).[34] This model revealed three distinct opportunities to disrupt DNA intercalation with our molecules. Namely, reducing the basicity of the amine functionality should disfavor the donation of hydrogen bonds to the DNA carbonyl. Second, growing toward, or shrinking from, the DNA backbone was predicted to disrupt the fit of our small molecules in DNA, leading to a less thermodynamically favorable interaction. Finally, introducing three-dimensionality could serve to disfavor the stabilizing pi-stack with DNA, mitigating the intercalation liability. We set out to test each of these hypotheses. Cognizant of the possibility that general cytotoxicity of molecules could confound comparisons across results from the mutagenicity assay, we also sought to develop an orthogonal higher throughput in vitro assay specific for DNA interaction.

We observed that the UV-Vis spectrum of some carboxamide compounds showed a saturable perturbation upon addition of duplex DNA, as reported for other organic ligands.[35] This facile assay allowed inhibitors to be tested prior to, or concurrent with, the TA97a mutagenicity assay, although the metabolic activation system (S9) could not be incorporated into the DNA interaction assay. To validate this approach, picolinamides **5** and **42** were profiled, and each showed positive data for DNA interaction, consistent with the mutagenicity results.[36] Further, metabolite **45** was negative in the UV-Vis assay, again matching the mutagenicity results for this

compound.[37] Of note, tricycle **44**, which was negative in the TA97a mutagenicity, was positive

for DNA interaction in the UV-Vis assay. Thus the UV-Vis assay can give false positive results

compared with the bacterial mutagenicity assay in TA97a (though the results may be more

robust, since cytotoxicity is not a confounder in this model), but we never observed a false

negative in this assay,[38] supporting its use as an orthogonal assessment of intercalation risk and

serving as a stage gate for the lower throughput bacterial mutagenicity assay.

Figure 9. Docking Model of Picolinamide **5** in DNA (from Acridine/DNA Co-Crystals).
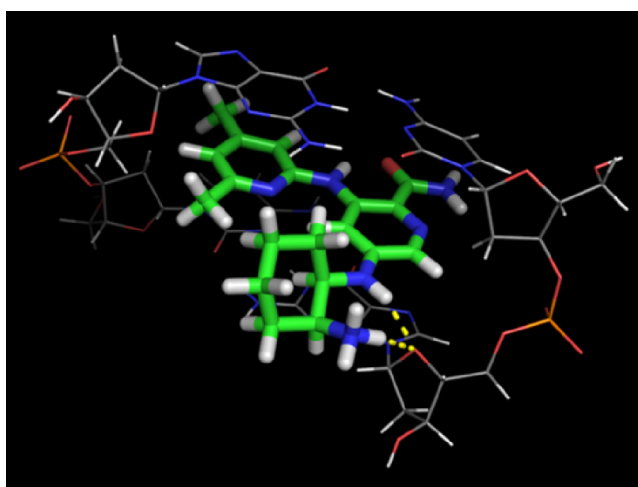
As shown in table 4, our first hypothesis regarding the attenuation of basicity still afforded

mutagenic/UV-Vis positive compounds (e.g. compound **48**). Ablating the basicity completely, as

in carboxamide **49**, afforded compounds predicted to lack intercalation, but at the expense of Syk

activity (Syk IC$_{50}$ = 60 nM). As previously detailed the basic amine interaction of our

carboxamide inhibitors with Asp-512 is a critical element for potency and selectivity on the

enzyme.

We next systematically surveyed substitution at the 4-, 5-, and 6-positions of the

aminopyridine projected toward solvent. Examples **50**, **51**, and **52** were selected to evaluate the

effectiveness of growing toward the DNA backbone to disrupt the fit of our inhibitors in DNA.

4-Substituted aliphatic alcohol **50** was negative in the TA97a mutagenicity assay, but positive in the UV-Vis assay. Of note, the compound could only be tested up to 1000 µg/plate in the bacterial assay, as higher concentration testing was precluded by general cytotoxicity. Pyrazole **51**, featuring a large substituent at the 5-position of the aminopyridine, which should be pointed directly at the DNA backbone, was negative in both the TA97a mutagenicity assay and UV-Vis assays while maintaining Syk potency (Syk IC$_{50}$ = 1 nM), representing a potential advance in our efforts. Growing from the 6-position of the aminopyridine, as in triazole **52**, gave very strong mutagenicity and UV-Vis positive results. Though we had gained some favorable data with pyrazole **51**, its physicochemical properties led to a particularly large cell shift (hWB CysLT IC$_{50}$/Syk IC$_{50}$ = 2800X for **51** versus 98X for **42**). Overall, the strategy of growing the molecule to mitigate mutagenicity did not seem the best path from an efficiency or physicochemical properties perspective, so we chose to prioritize alternative tactics.

Disruption of the pi stacking interaction with DNA was pursued via incorporation of sp^3 groups on the aminopyridine heterocycle (e.g. picolinamide **53**). Again, this strategy was not successful at overcoming intercalation in our hands, as carboxamide **53** was positive in both the mutagenicity and UV-Vis studies. Having pursued a number of paths with limited success, we decided to look at alternative substructures to mitigate the intercalation liability.
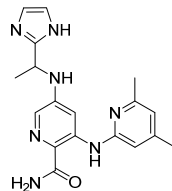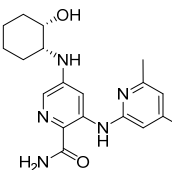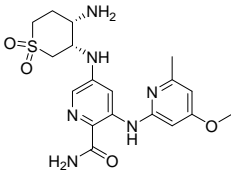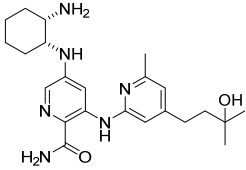
Further pursuing a change in the shape of the carboxamide chemotype to grow toward the DNA backbone and disfavor intercalation, we envisioned a carbon-link of the solvent group to the core carboxamide.[39] This design was applied to the synthesis of benzimidazole **54**, which demonstrated proof of concept for generation of a modestly potent/selective carbon-linked Syk inhibitor (Syk IC$_{50}$ = 7 nM, 97% of kinases >100X, 101 kinases tested, LRRK2 IC$_{50}$ = 130 nM, CHK2 IC$_{50}$ = 160 nM, TSSK3 IC$_{50}$ = 420 nM) that filled a different chemical space than the
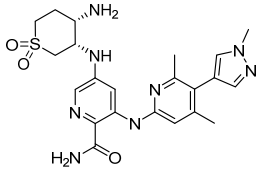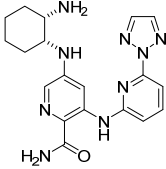
previous iteration of nitrogen-linked analogs (Figure 10).[40] We also pivoted this motif to pyrazinecarboxamide **55**, which delivered a highly favorable profile (Syk IC_{50} = 0.5 nM, 99% of kinases >100X, 101 kinases tested, LRRK2 IC_{50} = 30 nM, hWB CysLT IC_{50} = 130 nM, Rat Pla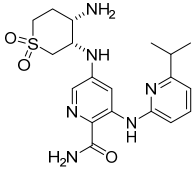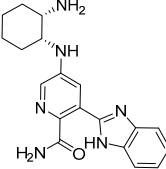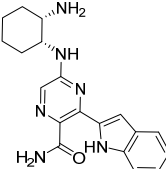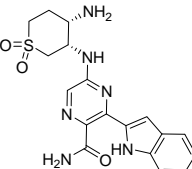sma Cl_p (Cl_u) = 44 (255) mL/min/kg, Rat $T_{1/2}$ = 2.8 h). Further, carboxamides **54** and **55** were negative in the UV-Vis assay for intercalation, and pyrazine **55** was also negative in the mutagenicity assay in strain TA97a with rat S9. Cyclohexyldiamine **55** was cytotoxic at concentrations greater than 850 μg/plate, so to mitigate cytotoxicity, the sulfonyldiamine analog **56**, was prepared. Pyrazine **56** was also negative in the UV-Vis assay, as well as the TA97a mutagenicity assay with rat S9, this time tested up to 5000 μg/plate. Delighted by these results, the team set out to further interrogate these findings and compare them in a third assay format. A DNA unwinding assay was utilized to study carboxamides **42**, **55**, and **56**; the results were in full agreement with the TA97a mutagenicity and UV-Vis assays, further supporting the viability of the carbon-linked motif as a method for obviating intercalation. Application of the design principles that had been used to overcome ion channel activity and mutagenicity afforded tetrahydropyranyldiamine **57** (Figure 11). Pyrazine **57** achieved the desired profile we had targeted from the outset with good intrinsic potency (Syk IC_{50} = 0.7 nM), high selectivity (99% of kinases >100X, 101 kinases tested, LRRK2 IC_{50} = 33 nM), potent cell functional activity (hWB CysLT IC_{50} = 62 nM) and a favorable pharmacokinetic profile in preclinical species (Rat Plasma Cl_p (Cl_u) = 25 (100) mL/min/kg, Rat $T_{1/2}$ = 3.5 h, 29 %F). Further, this molecule **57** posed low risk for ion channel activity and DNA interaction as assessed by our ion channel and UV-Vis displacement assays (hERG IC_{50} = 22 μM and UV-Vis = Negative).[41]

A recent report from the literature correlated Ames mutagenicity to a metric defined as "ovality" for a series of pyridazinecarboxamide Syk inhibitors.[25] Ovality was defined as the ratio

of the molecular surface area to the minimum surface area.[42] We attempted to retrospectively apply a similar calculation to test its predictivity for our studies. We found this metric to be highly sensitive to subtle changes in the geometry of the solvent front heteroaryl substituent. Across our data set, we observed no correlation between ovality and bacterial mutagenicity. As detailed, the key to circumvention of the mutagenicity issue in our case was a mechanistic understanding of the source of the liability (intercalation) along with testable design hypotheses to alter the shape of the carboxamide Syk inhibitors. We pursued both increasing the spherical nature of our molecules as well as two-dimensional perturbation of the spatial fit, ultimately affording the *C*-linked carboxamides that have shown no mutagenicity risk to date.

Table 4. Mutagenicity SAR.

Analog	Structure	Syk IC$_{50}$ (nM)[a]	Mutagenicity (µg/plate)[b]	UV-Vis[c]	DNA Unwinding[d]	Ovality[e]
48		51	Positive (1000)	Positive	ND	1.42
49		63	Negative (3000)	Negative	ND	1.42
42		0.6	Positive (1000)	Positive	Positive	1.39
50		0.4	Negative (1000)	Positive	ND	1.42

51		1	Negative (5000)	Negative	ND	1.47
52		0.1	Positive (300)	Positive	ND	1.39
53		2	Positive (300)	Positive	ND	1.36
54		7	ND	Negative	ND	1.34
55		0.5	Negative (850)	Negative	Negative	1.34
56		2.5	Negative (5000)	Negative	Negative	1.34

[a] [a]See supporting information for details. [b]Number represents highest scorable concentration for bacterial mutagenicity negative compounds and lowest concentration a positive score was achieved for positive compounds. [c]UV-Vis positive defined as $K_d \leq 500$ μM. [d]See supporting information for details and primary data. [e]Ovality calculated using a method adapted from the report by Lucas, M. C. et al.[25]

Figure 10. Overlay of *N*-linked Carboxamide (**42**, Red) with *C*-linked Carboxamide (**56**, Blue).
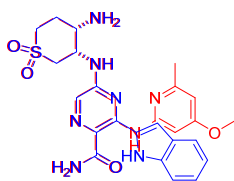
Figure 11. Profile of Pyrazine **57**.

Syk IC$_{50}$: 0.7 nM
hWB CysLT IC$_{50}$: 62 nM
Kinases >100X: 100% (100)
Rat Plasma Cl$_p$ (Cl$_u$): 25 (100) mL/min/kg
Rat T$_{1/2}$: **3.5 h, 29% F**
hERG IC$_{50}$: 22 µM
UV-Vis Displacement: Negative

57
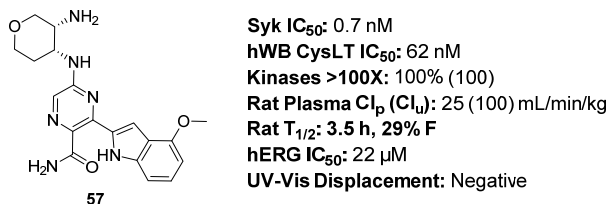
Conclusions

A novel series of orally efficacious, selective carboxamide Syk inhibitors were discovered via systematic survey of chemotypes prioritized by ligand efficiencies and structural alerts. The critical basic amine functionality of the 3,5-diamino picolinamides afforded undesired hERG ion channel activity, which was mitigated via modulation of physicochemical properties. PSA emerged as the most effective calculated property in circumventing hERG activity and was used to prospectively design Syk inhibitors devoid of this liability. A mutagenicity risk was subsequently discovered within these chemotypes. The mechanism for mutagenesis was identified as involving intercalation. Several structure-based design hypotheses were interrogated to obviate this issue; modulation of the two-dimensional shape of the molecules led to the identification of an alternative series of *C*-linked heterocyclic carboxamides, delivering drug-like molecules devoid of hERG ion channel activity, mutagenicity, and intercalation risk, while maintaining Syk potency and selectivity.

ASSOCIATED CONTENT

Supporting Information.

Experimental procedures for synthesis of final compounds and intermediates, and descriptions of assays performed. This material is available free of charge via the Internet at http://pubs.acs.org.

AUTHOR INFORMATION

Corresponding Author

*Phone: +1-617-992-3144; e-mail: michael_ellis@merck.com

Present Addresses

*J. Michael Ellis: Merck Research Laboratories, 33 Avenue Louis Pasteur, Boston, MA 02115, United States

Notes

The authors declare no competing financial interest.

ABBREVIATIONS

Syk, Spleen tyrosine kinase; RA, rheumatoid arthritis; DMARD, disease-modifying antirheumatic drug; Fc, fragment, crystallizable; BCR, B cell receptor; Syk IC_{50}, recombinant human Syk IC_{50}; LBE, ligand binding efficiency; hWB, human whole blood; MetID, metabolite

identification; S$_N$Ar, nucleophilic aromatic substitution; MeOH, methanol; DIEA, *N,N*-diisopropylethylamine; NIS, *N*-iodosuccinimide.

REFERENCES

(Word Style "TF_References_Section"). References are placed at the end of the manuscript. Authors are responsible for the accuracy and completeness of all references. Examples of the recommended format for the various reference types can be found at http://pubs.acs.org/page/4authors/index.html. Detailed information on reference style can be found in *The ACS Style Guide,* available from Oxford Press.

[1] Cohen, M. H.; Williams, G.; Johnson, J. R.; Duan, J.; Gobburu, J.; Rahman, A.; Benson, K.; Leighton, J.; Kim, S. K.; Wood, R.; Rothmann, M.; Chen, G.; Maung U, K.; Staten, A. M.; Pazdur, R. Approval summary for imatinib mesylate capsules in the treatment of chronic myelogenous leukemia. *Clin. Cancer Res.* **2002**, *8*, 935–942.

[2] Bonilla-Hernán, M. G.; Miranda-Carús, M. E.; Martin-Mola, E. New drugs beyond biologics in rheumatoid arthritis: the kinase inhibitors. *Rheumatology* **2011**, *50*, 1542–1550.

[3] Müller-Ladner, U.; Pap, T.; Gay, R. E.; Neidhart, M.; Gay S. Mechanisms of Disease: the molecular and cellular basis of joint destruction in rheumatoid arthritis. *J. Clin. Pract. Rheumatol.* **2005**, *1*, 102–110.

[4] Filer, A.; Parsonage, G.; Smith, E.; Osborne, C.; Thomas, A. M.; Curnow, S. J.; Rainger, G. E.; Raza, K.; Nash, G. B.; Lord, J.; Salmon, M.; Buckley, C. D. Differential survival of

leukocyte subsets mediated by synovial, bone marrow, and skin fibroblasts: site-specific versus activation-dependent survival of T cells and neutrophils. *Arthritis Rheum.* **2006**, *54*, 2096–2108.

[5] Nimmerjahn, F.; Ravetch, J. V. Fcγ receptors as regulators of immune responses. *Nat. Rev. Immunol.* **2008**, *8*, 34–47.

[6] Burmester G.R.; Blanco, R.; Charles-Schoeman, C.; Wollenhaupt, J.; Zerbini, C.; Benda, B.; Gruben, D.; Wallenstein, G.; Krishnaswami, S.; Zwillich, S. H.; Koncz, T.; Soma, K.; Bradley, J.; Mebus, C. Tofacitinib (CP-690,550) in combination with methotrexate in patients with active rheumatoid arthritis with an inadequate response to tumour necrosis factor inhibitors: a randomised phase 3 trial. *Lancet* **2013**, *381*, 451–460.

[7] Geahlen, R. L. Getting Syk: spleen tyrosine kinase as a therapeutic target. *Trends Pharmacol. Sci.* **2014**, *35*, 414–422.

[8] Mocsai, A.; Ruland, J.; Tybulewicz, V. L. J. The Syk tyrosine kinase: a crucial player in diverse biological functions. *Nat. Rev. Immunol.* **2010**, *10*, 387–402.

[9] Pine, P. R.; Chang, B.; Schoettler, N.; Banquerigo, M. L.; Wang, S.; Lau, A.; Zhao, F.; Grossbard, E. B.; Payan, D. G.; Brahn, E. Inflammation and bone erosion are suppressed in models of rheumatoid arthritis following treatment with a novel Syk inhibitor. *Clin. Immunol.* **2007**, *124*, 244−257.

[10] Coffey, G.; DeGuzman, F.; Inagaki, M.; Pak, Y.; Delaney, S. M.; Ives, D.; Betz, A.; Jia, Z. J.; Pandey, A.; Baker, D.; Hollenbach, S. J.; Phillips, D. R.; Sinha, U. Specific inhibition of

1
2
3
4
5
6
7
8
9
10

spleen tyrosine kinase suppresses leukocyte immune function and inflammation in animal models of rheumatoid arthritis. *J. Pharmacol. Exp. Ther.* **2012**, *340*, 350−359.

[11] Liao, C.; Hsu, J.;Kim, Y.; Hu, D.-Q.; Xu, D.; Zhang, J.; Pashine, A.; Menke, J.; Whittard, T.; Romero, N.; Truitt, T.; Slade, M.; Lukacs, C.; Hermann, J.; Zhou, M.; Lucas, M.; Narula, S.; DeMartino, J.; Tan, S.-L. Selective inhibition of spleen tyrosine kinase (SYK) with a novel orally bioavailable small molecule inhibitor, RO9021, impinges on various innate and adaptive immune responses: implications for SYK inhibitors in autoimmune disease therapy. *Arthritis Res. Ther.* **2013**, *15*, R146.

[12] Currie, K. S.; Kropf, J. E.; Lee, T.; Blomgren, P.; Xu, J.; Zhao, Z.; Gallion, S.; Whitney, J. A.; Maclin, D.; Lansdon, E. B.; Maciejewski, P.*;* Rossi, A. M.; Rong, H.; Macaluso, J.; Barbosa, J.; Di Paolo, J. A.; Mitchell, S. A. Discovery of GS-9973, a selective and orally efficacious inhibitor of spleen tyrosine kinase. *J. Med. Chem.* **2014**, *57*, 3856–3873.

[13] Weinblatt, M. E.; Kavanaugh, A.; Genovese, M. C.; Jones, D. A.; Musser, T. K.; Grossbard, E. B.; Magilavy, D. B. Effects of fostamatinib (R788), an oral spleen tyrosine kinase inhibitor, on health-related quality of life in patients with active rheumatoid arthritis: analyses of patient-reported outcomes from a randomized, double-blind, placebo-controlled trial. *J. Rheumatol.* **2013**, *40*, 369–378.

[14] Edwards J.; Szczepanski, L.; Szechinski, J.; Filipowicz-Sosnowska, A.; Emery, P.; Close, D.; Stevens, R.; Shaw, T. Efficacy of B-cell-targeted therapy with rituximab in patients with rheumatoid arthritis. *N. Engl. J. Med.* **2004**, *350*, 2572–81.

[15] For the role of VEGF inhibition in hypertension see: Pande, A.; Lombardo, J.; Spangethal, E.; Javle, M. Hypertension secondary to anti-angiogenic therapy: experience with bevacizumab. *Anticancer Res.* **2007**, *27*, 3465–3470.

[16] Suljagic, M.; Longo, P. G.; Bennardo, S.; Perlas, E.; Leone, G.; Laurenti, L.; Efremov, D. G. The Syk inhibitor fostamatinib disodium (R788) inhibits tumor growth in the Eμ-TCL1 transgenic mouse model of CLL by blocking antigen-dependent B-cell receptor signaling. *Blood* **2010**, *116*, 4894–4905.

[17] Friedberg, J. W.; Sharman, J.; Sweetenham, J.; Johnston, P. B.; Vose, J. M.; Lacasce, A.; Schaefer-Cutillo, J.; De Vos, S.; Sinha, R.; Leonard, J. P.; Cripe, L. D.; Gregory, S. A.; Sterba, M. P.; Lowe, A. M.; Levy, R.; Shipp, M. A. Inhibition of Syk with fostamatinib disodium has significant clinical activity in non-Hodgkin lymphoma and chronic lymphocytic leukemia. *Blood* **2010**, *115*, 2578–2585.

[18] Ulanova, M.; Duta, F.; Puttagunta, L.; Schreiber, A. D.; Befus, A. D. Spleen tyrosine kinase (Syk) as a novel target for allergic asthma and rhinitis. *Expert Opin. Ther. Targets* **2005**, *9*, 901–921.

[19] Moy, L. Y.; Jia, Y.; Caniga, M.; Lieber, G.; Gil, M.; Fernandez, X.; Sirkowski, E.; Miller, R.; Alexander, J. P.; Lee, H.-H.; Shin, J. D.; Ellis, J. M.; Chen, H.; Wilhelm, A.; Yu, H.; Vincent, S.; Chapman, R. W.; Kelly, N.; Hickey, E.; Abraham, W. M.; Northrup, A.; Miller, T.; Houshyar, H.; Crackower, M. A. Inhibition of spleen tyrosine kinase attenuates allergen-mediated airway constriction. *Am. J. Respir. Cell. Mol. Biol.* **2013**, *49*, 1085–1092.

20 Surry, D. S.; Buchwald, S. L. Dialkylbiaryl phosphines in Pd-catalyzed amination: a user's guide. *Chem. Sci.* **2011**, *2*, 27–50.

21 Miyaura, N.; Yamada, K.; Suzuki, A. A new stereospecific cross-coupling by the palladium-catalyzed reaction of 1-alkenylboranes with 1-alkenyl or 1-alkynyl halides. *Tetrahedron Lett.* **1979**, *36*, 3437–3440.

22 Hisamichi, H.; Naito, R.; Toyoshima, A.; Kawano, N.; Ichikawa, A.; Orita, A.; Orita, M.; Hamada, N.; Takeuchi, M.; Ohta, M.; Tsukamoto, S. Synthetic studies on novel Syk inhibitors. Part 1: Synthesis and structure-activity relationships of pyrimidine-5-carboxamide derivatives. *Bioorg. Med. Chem.* **2005**, *13*, 4936–4951.

23 Villasenor, A.G., Kendra, R., Ho, H., Wang, S., Papp, E., Shaw, D., Barnett, J.W., Browner, M.F., Kuglstatter, A. Structural insights for design of potent spleen tyrosine kinase inhibitors from crystallographic analysis of three inhibitor complexes. *Chem. Biol. Drug Des.* **2009**, *73*, 466–470.

24 Stepan, A. F.; Walker, D. P.; Bauman, J.; Price, D. A.; Baillie, T. A.; Kalgutkar, A. S.; Aleo, M. D. Structural alert/reactive metabolite concept as applied in medicinal chemistry to mitigate the risk of idiosyncratic drug toxicity: a perspective based on the critical examination of trends in the top 200 drugs marketed in the United States. *Chem. Res. Toxicol.* **2011**, *24*, 1345–1410.

25 Data for pyridazinecarboxamide **21** from Lucas, M. C.; Bhagirath, N.; Chiao, E.; Goldstein, D. M.; Hermann, J. C.; Hsu, P.-Y.; Kirchner, S.; Kennedy-Smith, J. J.; Kuglstatter, A.; Lukacs, C.; Menke, J.; Niu, L.; Padilla, F.; Peng, Y.; Polonchuk, L.; Railkar, A.; Slade, M.; Soth, M.; Xu, D.; Yadava, P.; Yee, C.; Zhou, M.; Liao, C. Using ovality to predict nonmutagenic, orally

efficacious pyridazine amides as cell specific spleen tyrosine kinase inhibitors. *J. Med. Chem.* **2014**, *57*, 2683–2691.

[26] This level of Zap70 versus Syk enzymatic selectivity was generally maintained for all carboxamides.

[27] Lipinski, C. A. Drug-like properties and the causes of poor solubility and poor permeability. *J. Pharmacol. Toxicol.* **2000**, *44*, 235–249.

[28] Jamieson, C.; Moir, E. M.; Rankovic, Z.; Wishart, G. Medicinal Chemistry of hERG Optimizations: Highlights and Hang-Ups. *J. Med. Chem.* **2006**, *49*, 5029–5046.

[29] Wang, J.; Della Penna, K.; Wang, H.; Karczewski, J.; Connolly, T. M.; Koblan, K. S.; Bennett, P. B.; Salata, J. J.; Functional and pharmacological properties of canine ERG potassium channels. *Am. J. Physiol.* **2003,** *284*, 256–267.

[30] Higher throughput binding assay measures displacement of MK-499, a strong binder to the hERG ion channel. Priest, B. T.; Bell, I. M.; Garcia, M. L. Role of hERG potassium channel assays in drug development. *Channels* **2008**, *2*, 87–93.

[31] Kawai, Y.; Tsukamoto, S.; Ito, J.; Akimoto, K.; Takahashi, M. A risk assessment of human ether-a-go-go-related gene potassium channel inhibition by using lipophilicity and basicity for drug discovery. *Chem Pharm Bull (Tokyo)* **2011**, *59*, 1110–1116.

[32] Liddle, J.; Atkinson, F. L.; Barker, M. D.; Carter, P. S.; Curtis, N. R.; Davis, R. P.; Douault, C.; Dickson, M. C.; Elwes, D.; Garton, N. S.; Gray, M.; Hayhow, T. G.; Hobbs, C. I.; Jones, E.; Leach, S.; Leavens, K.; Lewis, H. D.; McCleary, S.; Neu, M.; Patel, V. K.; Preston, A. G. S.;

Ramirez-Molina, C.; Shipley, T. J.; Skone, P. A.; Smithers, N.; Somers, D. O.; Walker, A. L.; Watson, R. J.; Weingarten, G. G. Discovery of GSK143, a highly potent, selective and orally efficacious spleen tyrosine kinase inhibitor. *Bioorg. Med. Chem. Lett.* **2011**, *21*, 6188–6194.

[33] http://www.ich.org/fileadmin/Public_Web_Site/ICH_Products/Guidelines/Safety/S2_R1/Step4/S2R1_Step4.pdf

[34] Adams, A., Guss, J.M., Denny, W.A., Wakelin, L.P. Crystal structure of 9-amino-N-[2-(4-morpholinyl)ethyl]-4-acridinecarboxamide bound to d(CGTACG)2: implications for structure-activity relationships of acridinecarboxamide topoisomerase poisons. *Nucleic Acids Res.* **2002**, *30*, 719–725.

[35] Zang, H.; Gates, K. S. DNA binding and alkylation by the "left half" of azinomycin B. *Biochem.* **2000**, *39*, 14968–14975.

[36] Doxorubicin, a known intercalator, was titrated as a positve control for this assay. Structurally diverse Syk inhibitors were used as negative controls. See Northrup, A. B.; Altman, M. D.; Andresen, B. M.; Anthony, N. J.; Arrington, K. L.; Bhat, S.; Bienstock, C. E.; Black, C.; Burch, J.; Butcher, J. W.; Childers, K. K.; Cote, B.; Deschenes, D.; di Francesco, E.; Donofrio, A.; Ducharme, Y.; Dupont-Gaudet, K.; Ellis, J. M.; Fischer, C.; Fournier, J.-F.; Friesen, R.; Gauthier, J. Y.; Grimm, J. B.; Guay, D.; Guerin, D. J.; Haidle, A. M.; Jewell, J. P.; Kattar, S. D.; Li, C.; Lim, J.; Lee, S.; Liu, Y.; Machacek, M. R.; Maddess, M. L.; Miller, T. A.; O'Boyle, B. M.; Otte, R. D.; Peterson, S. L.; Petrocchi, A.; Reutershan, M. H.; Romeo, E. T.; Robichaud, J. S.; Schell, A. J.; Siu, T.; Smith, G. F.; Spencer, K. B.; Taoka, B. M.; Trotter, B. W.; Yang, L.;

Woo, H. C.; Zhou, H. *Abstracts of Papers*, 247th ACS National Meeting & Exposition, Dallas, TX, March 16-20, 2014; American Chemical Society: Washington, DC, 2014; MEDI-36.

[37] All compounds tested to a top concentration of 406 μM DNA. See supporting information for further details.

[38] 10 of 30 compounds tested were negative in the UV-Vis and bacterial mutagenicity assays.

[39] A detailed account of the design principles applied to this scaffold re-design will be the subject of a future communication.

[40] X-ray crystallograhpic data for the *C*-linked carboxamides will be detailed in a future communication.

[41] We note that pyrazine **57** has not been tested in TA97a or the other strains used in the Ames bacterial mutagenicity assay.

[42] The minimum surface area is the surface area of a sphere having a volume equal to the solvent-excluded volume of the molecule (computed from the Connolly molecular surface area and solvent-excluded volume properties).

1
2
3
4
5
6
7
8
9
10
11
12
13
14
15
16
17
18
19
20
21
22
23
24
25
26
27
28
29
30
31
32
33
34
35
36
37
38
39
40
41
42
43
44
45
46
47
48
49
50
51
52
53
54
55
56
57
58
59
60

Table of Contents graphic

Physicochemical property modulation

rhSyk IC$_{50}$: 0.06 nM
LE: 0.56
hERG IC$_{50}$: 1.6 μM

Scaffold re-design/ shape change

rhSyk IC$_{50}$: 0.6 nM
LE: 0.44
hERG IC$_{50}$: >30 μM
Mutagenicity: Positive

rhSyk IC$_{50}$: 2 nM
LE: 0.42
hERG IC$_{50}$: >30 μM
Mutagenicity: Negative